Molecular Crystals and Liquid Crystals
Publication details, including instructions for authors and subscription information:
http://www.tandfonline.com/loi/gmcl20

The Dominance of Morphology over Size in the Decrease of the Activation Energy of Biphase TiO_2 Nanocrystallites

Hossain Milani Moghaddam [a b d] & Shahruz Nasirian [a b c]

[a] Department of Physics, University of Mazandaran, Babolsar, Iran

[b] Molecular Electronics Lab., Department of Physics, University of Mazandaran, Babolsar, Iran

[c] Department of Basic Sciences, University of Science & Technology of Mazandaran, Babol, Iran

[d] Nano and Biotechnology group, University of Mazandaran, Babolsar, Iran

Version of record first published: 30 Jul 2012.

To cite this article: Hossain Milani Moghaddam & Shahruz Nasirian (2012): The Dominance of Morphology over Size in the Decrease of the Activation Energy of Biphase TiO_2 Nanocrystallites, Molecular Crystals and Liquid Crystals, 562:1, 219-228

To link to this article: http://dx.doi.org/10.1080/10426507.2012.669676

Mol. Cryst. Liq. Cryst., Vol. 562: pp. 219–228, 2012

ISSN: 1542-1406 print/1563-5287 online
DOI: 10.1080/10426507.2012.669676

The Dominance of Morphology over Size in the Decrease of the Activation Energy of Biphase TiO_2 Nanocrystallites

HOSSAIN MILANI MOGHADDAM[1,2,4,*]
AND SHAHRUZ NASIRIAN[1,2,3]

[1]Department of Physics, University of Mazandaran, Babolsar, Iran
[2]Molecular Electronics Lab., Department of Physics, University of Mazandaran, Babolsar, Iran
[3]Department of Basic Sciences, University of Science & Technology of Mazandaran, Babol, Iran
[4]Nano and Biotechnology group, University of Mazandaran, Babolsar, Iran

Single-phase and biphase TiO_2 nanoparticles have been prepared by the sol-gel method. Our results showed with the increase of the gelatinization time and the calcination, the size of initial anatase particles and the size of final biphase particles were increased; however, distortion and agglomeration of both of TiO_2 nanoparticles were decreased. Moreover, the mass fraction of rutile (MFR) phase and the activation energy of the phase transformation (PT) from anatase to rutile decrease. We demonstrated that the morphology and homogeneity of the initial anatase nanoparticle could have more important than its initial size to appear the lower activation energy.

Keywords Activation energy; phase transformation; sol-gel method; titanium dioxide nanocrystallites

Introduction

Natural polymorphs of TiO_2 are known to exist as rutile and anatase and brookite. Different applications of TiO_2 have been found to depend strongly on the crystalline structures morphology and particle size [1–7]. For instance, rutile phase is used as a white pigment, a coating material for optical lenses due to its effective light scattering, dielectric gate material for field emission transistor devices as a result of its high dielectric constant (>100) [7,8] and gas sensor due to the dependence of the electric conductivity on the ambient gas composition [9]. Moreover, anatase phase is used as an anode material in which lithium ions can intercalate reversibly [10], photocatalysts [2–6], ultraviolet filters for optics, and packing materials [11].

In view of the synthetic methods and application materials, Zhang et al. [12], Shen et al. [13], Zumeta et al., [14] and Carp et al. [2] have reported that the photocatalytic and photovoltaic properties of TiO_2 with two different phases of anatase (70%–75%) and

*Address correspondence to Hossain Milani Moghaddam, Code: 47416-95447, Faculty of Basic Sciences, University of Mazandaran, Beheshti St., Babolsar, Iran. E-mail: milani@umz.ac.ir; hossainmilani@yahoo.com

rutile (30%–25%) are better than pure anatase or rutile TiO_2 nanoparticles. The mixtures of anatase and rutile have recently been fabricated by chemical and physical methods, including a solvothermal, hydrothermal, ultrasonic irradiation and sol-gel [1–3,15]. Anatase is metastable phase and the phase normally found in the sol-gel route of TiO_2 nanoparticles [15,16]. As usual, the preparation of the biphase (anatase-rutile) TiO_2 nanoparticles needs to crystallize the as-prepared titanium hydroxide at high temperature ($\geq$500°C). The actual transformation behavior for the preparation of biphase TiO_2 depends on initial particle size, impurity content, starting phase, and calcination temperature. Furthermore, the activation energy has an important role in the phase transformation (PT). The alteration of initial particle size and morphology can be changing the activation energy required for the PT from anatase to rutile (AEPT). Li et al. [17] reported that, AEPT, transition onset point (TOP) was decreased and the mass fraction of rutile (MFR) was increased with the decrease of initial size of anatase TiO_2 nanoparticles, even if distortion existed in sample. But they did not study the role of the morphology of initial anatase TiO_2 nanoparticles on AEPT, TOP, and MFR.

The preparation of TiO_2 mixed phase with lower AEPT will be useful both in saving energy and getting better properties. Therefore, further studies are still necessary in order to get a better understanding of the impact of size and morphology on AEPT. There is no report, known to us, which studied the effect of the gelatinization time and the calcinations on the morphology of the initial nanoparticles for PT and AEPT. In this paper, we have tried to control AEPT of TiO_2 nanopowders and to obtain a mixed phase of titanium dioxide. In addition, the effects of different parameters such as the morphology and the initial crystallite size due to the alteration of the gelatinization time and the calcination of the sol-gel route on PT of prepared TiO_2 nanoparticles have been discussed.

Experimental Details

Materials and Synthesis of TiO_2 Nanoparticles

The 5.0 ml titanium tetrachloride (99.5% Merck) was dropped into 50 ml ethanol (99.8% Merck) under vigorous stirring and argon gas environment until the yellowish solution disappeared. The pH of the final solution was approximately 1.0–1.5. The solution was mixed in several times (as 24, 72, and 120 hours) under humid air atmosphere with 88% humidity and temperature of 22°C. After the formation of the sol-gel, each prepared solution putted in the aging process up to 3–5 hours. We then prepared each gel solution with using ultrasonic waves with a frequency of 40 kHz and 60 Watt power for 30 min. Each sol-gel solution was vaporized at 80°C in environmental conditions, until a dry-gel was obtained. The dry-gel was dried overnight in an oven at 120°C. The TiO_2 powders were grounded using mortar and pestle. The as-prepared sample was thermally treated at the temperature rang 300°C to 900°C for 1 hour at each temperature. The thermal treatment was carried out in a convention electrical resistance furnance (Carbolite, England) under an ambient atmosphere at a rate of 5°C min^{-1}.

Characterization of TiO_2 Nanostructures

X-ray diffraction (XRD) at 30 kV was used to identify the crystalline phases and to estimate the crystallite size. The XRD patterns were recorded with 2θ in the range of 10°–80° by step scanning, using 2θ increments of 0.02° and a fixed counting time of 5 sec $step^{-1}$, with a GBC-MMR, employing Cu-K_α radiation. Scanning electron microscopy (SEM)

with type Philips-XL30 at 16 kV and transmission electron microscopy (TEM) with type Phillips CM-120 at 100 kV were used to further examine the crystallite (particle) size, the crystallinity and morphology of the as-synthesized TiO_2 samples.

Results and Discussion

SEM and TEM Characterization

Figure 1 shows SEM images taken from TiO_2 powder samples at a calcination temperature of 500°C and the gelatinization time of (a) 24 hours and (b) 120 hours. The nanoparticles were agglomerated and poorly crystallized at a low gelatinization time. These images obviously showed high homogeneity and good morphology of the samples had strongly dependent on the gelatinization time. Figure 2 shows the TEM micrographs taken from powder samples made with the gelatinization time of 120 hours and calcined at 300°C and 500°C. After being thermally treated at 300°C for 1 hour, loosely aggregated nanoparticles with the nonhomogeneous particle were observed and the dispersivity and homogeneity of the particles was not good [Fig. 2(a)]. In this case, the nanoparticles were strongly agglomeration. After a further calcination at 500°C for 1 hour, the anatase TiO_2 nanoparticles were nearly spherical and the size of about 20 ± 5 nm. According to Fig. 2(b), the nanoparticles had a good homogeneity and an appropriate morphology. As a result, the as-prepared powder in the lower/higher calcination consisted of particles with a high/low agglomeration.

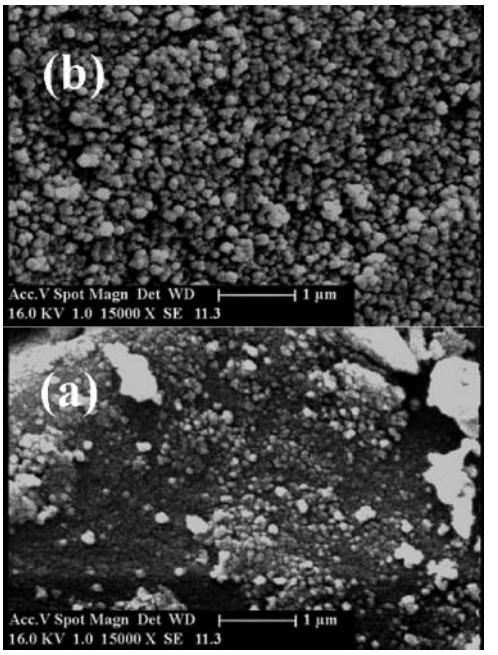

Figure 1. SEM images of samples calcined at 500°C for 1 hour. The sol-gel solution mixed for (a) 24 hours and (b) 120 hours.

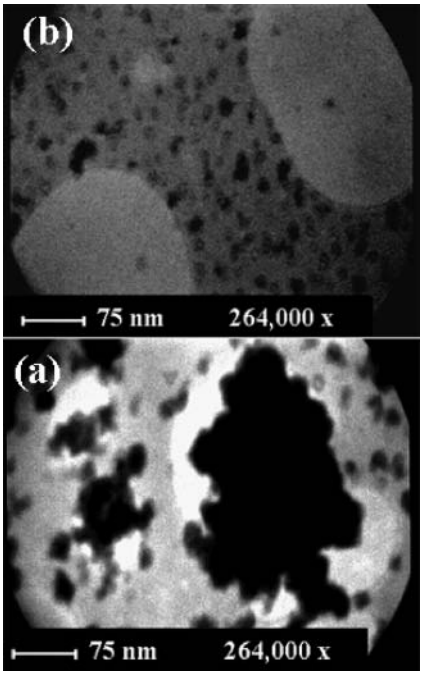

Figure 2. TEM images of the gelatinized samples for 120 hours and calcined after 1 hour at (a) 300°C and (b) 500°C.

XRD Characterization

The XRD patterns of the as-prepared samples obtained at different experimental conditions are shown in Fig. 3. Figures 3(a), 3(b), and 3(c) show in a calcination step at temperature ranging from 400°C to 500°C, the crystallinity improved with the decrease of broadening of the XRD peaks of anatase phase (101). There were not also any corresponding peaks to confirm the crystallization of rutile or brookite in this temperature range. When the calcination increased from 500°C to 550°C, the anatase-rutile transformation appeared and it preceded and completed primarily in the powders with the lowest gelatinization time. At the calcination temperature from 550°C to 750°C, observing that the intensity of the rutile peak increased significantly while the intensity of the anatase peak decreased.

When the samples calcined at 900°C, the anatase peak (101) disappeared and a single rutile phase was observed in the gelatinization time of 24 hours and a little intensity of the anatase peak was observed in the gelatinization time of 72 hours and 120 hours.

The average crystallite size (D) was calculated from full width at half-maximum (FWHM) according to Debby–Scherrer's formula [18] (as shown in Table 1):

$$D = 0.9\lambda/(\beta_{hkl}.\cos\theta_{hkl}) \tag{1}$$

where λ is the wavelength of the X-ray radiation (0.1541 nm), θ_{hkl} is the Bragg's angle in degree. β_{hkl} is the full width at half maximum (FWHM) of the peak.

According to Table 1, both anatase and rutile particle sizes increased with the increase of the calcination and the gelatinization time at ranging from 400°C to 750°C and from 24 hours to 120 hours, respectively. In spite of the fact that the size of the anatase nanoparticles

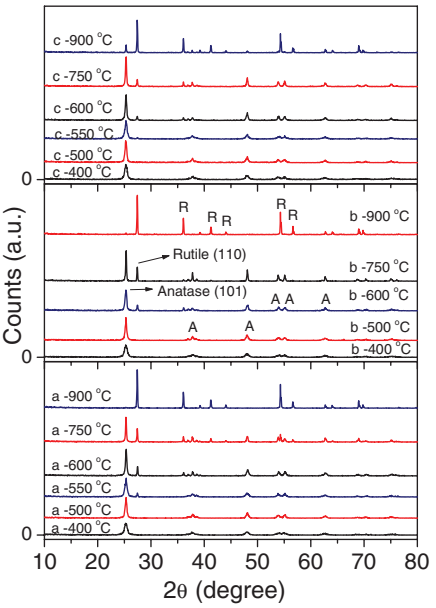

Figure 3. XRD patterns of TiO_2 nanopowder calcined at different temperatures and gelatinized in (a) 24 hours, (b) 72 hours, and (c) 120 hours; (A: anatase, R: rutile).

continued to grow, the size of the rutile particles remained fixing at the temperature ranging from 750°C to 900°C. Nevertheless, the decrease in the size of anatase particles was observed at calcination of 550°C and each gelatinization time that, maybe, because of the beginning of PT. Therefore, the small broadening of XRD peaks sequence after the heat treatment was attributed to an increase in the crystalline size, indicating that the amount of rutile formed depended on the gelatinization time of the solution, the calcination temperature and the average crystallite size of the initial anatase phase. The results of XRD patterns were in good accordance with the results of SEM and TEM images.

MFR and AEPT

If a sample contains only anatase and rutile, the phase content of a sample can be calculated from the integrated intensities of anatase and rutile peaks. MFR (X_R) was calculated from the formula [17,19].

$$X_R = \left[1 + 0.8\left(\frac{I_A}{I_R}\right)\right]^{-1} \tag{2}$$

where I_A and I_R are the integrated intensity of anatase (101) and rutile (110) peaks, respectively.

MFR at different experimental conditions was calculated and the results shown in Table 1. Based on the results of MFR, we obtained the best combination, according to refs. [12–14] from the view of photocatalytic and photovoltaic properties, of anatase (70%–75%)-rutile (30%–25%) at the calcination of 750°C and various gelatinization times.

Figure 4 shows the phase contents of rutile in samples which were treated isochronally at 1 hour in the temperature range 550°C–900°C. The growth of rutile phase was also

Table 1. The size of nanocrystalline and MFR at different experimental conditions

	Gelatinizing time (hours)								
	24			72			120		
Calcination temperature (°C)	Anatase (101) crystalline size (nm)	Rutile (110) crystalline size (nm)	X_R (%)	Anatase (101) crystalline size (nm)	Rutile (110) crystalline size (nm)	X_R (%)	Anatase (101) crystalline size (nm)	Rutile (110) crystalline size (nm)	X_R (%)
400	12.15	0	0	14.01	0	0	14.8	0	0
500	20.1	0	0	23	0	0	24.3	0	0
600	28	34	18.1	30.1	35.5	17.9	32.6	34.1	17.3
750	37.9	52.7	31	40.7	52.7	27.6	42.9	49.5	25.2
900	0	54.7	100	0	54.7	100	58.3	56.4	83.3

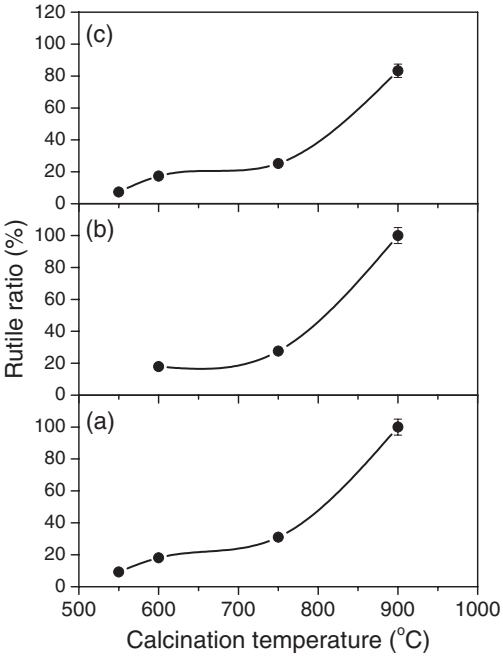

Figure 4. Evolution of the amount of Rutile phases in the various calcinations. The samples gelatinized in (a) 24 hours, (b) 72 hours, and (c) 120 hours.

better in the gelatinization process for 24 hours because of the smaller crystallite size of the initial anatase TiO_2. At the same time, temperature controlled heat and mass transportation causes anatase to grow by merging other anatase particles although its net amount was diminishing. Therefore, it was easier to overcome the energy barrier to start the nucleation of a new phase for TiO_2 nanoparticles with smaller sizes compared to the larger particles because more free surface area and interface can be provided in smaller particles for the rutile formation. Moreover, anatase/rutile got packed and became denser toward the interior of the particles as the growth of the anatase (A) phase itself and the concurrent growth of the rutile (R) phase proceeded [17,20,21].

The reaction rate for this transformation demonstrated that there must be lots of nucleation and growth site for transformation and also there was high driving force for the transition (free energy change for PT). In summary, the main factor determining the rate for transformation of phase A to phase R by a nucleation and growth mechanism was $\Delta G_{A\rightarrow R}$, which is the difference in free energy between A and R. So, it seems that the free energy between anatase and rutile phase in transformation of the samples that drived in the high gelatinization time was low. So, to clarify this inference, we have calculated AEPT using Avrami and Arrhenius equations. It has been shown that kinetics of PT is followed by Avrami formula as follows [20].

$$X_R = 1 - \exp(-k.t) \tag{3}$$

where t and k are the time and the kinetic constant, respectively. The kinetic constant can be calculated for each transformation fraction. AEPT can be obtained according to the

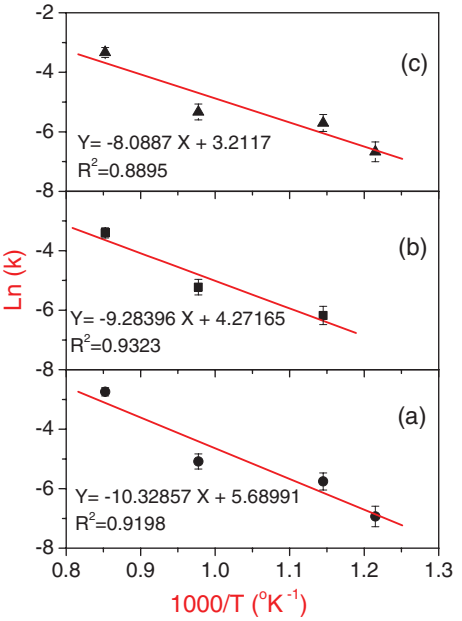

Figure 5. Arrhenius plots for samples obtained at different times; as (a) 24 hours, (b) 72 hours, and (c) 120 hours.

Arrhenius formula [17,19,20].

$$\mathrm{Ln}(k) = (-E_a/\mathrm{RT}) + \mathrm{Ln}(k_\circ) \tag{4}$$

where $k_\circ$, E_a, T, and R are a material properties constant, the activation energy, the temperature in Kelvin, and the universal gas constant (8.314 J $\mathrm{mol}^{-1\circ}\mathrm{K}^{-1}$), respectively.

From the Arrhenius plots of various kinetic constants for the as-prepared samples obtained at different experimental conditions (Fig. 5) and with the calculation of slop, the activation energy was obtained as 85.87, 77.19, and 67.25 k J mol^{-1}, when the samples mixed for 24, 72, and 120 hours and calcined at different temperatures, respectively.

Figure 6 shows the activation energy vs. the gelatinizing time. In this figure, there is a linear relationship between increasing gelatinization time and decreasing activation energy. AEPT also decreased with the increase of the gelatinization time. As a result, TOP was decreased with the decrease of the size of the initial anatase crystallite; however, the activation energy was increased.

This is not in relative agreement with the reported results by Li et al. [17], who have concluded that only the size of the initial anatase nanoparticle was the main factors in AEPT. They did not report the importance role of morphology of the initial TiO_2 nanoparticles in PT. Apparently, distortions, agglomeration and homogeneity effects have more important in the decrease of AEPT.

The homogeneity of the samples was better; however, distortions and agglomeration of the samples were less when the gelatinization time or the calcination temperature increased (as shown in SEM, TEM, and XRD results). Thus, the decrease of the average size of the initial anatase nanoparticles was an important factor for the decrease of TOP. We suggest

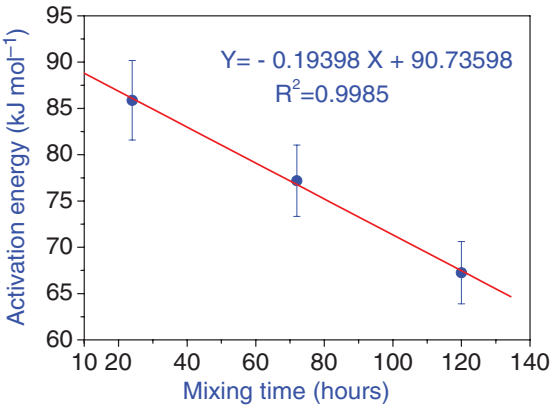

Figure 6. The activation energy vs. the gelatinization time for samples obtained at different experimental conditions.

that a good morphology and low distribution of the anatase nanoparticles were another important factor that has contributed in the decrease of AEPT.

Conclusion

Nanocrystalline anatase and/or rutile (TiO_2) were prepared from stable sols produced using low-cost method of sol-gel by two main mechanisms; via controlling the gelatinization time and calcination temperatures. Our results showed that anatase was only phase in titanium dioxide powders up to 500°C and when the calcination increased in the region after 500°C, PT happened in TiO_2 nanopowders and biphase occurred. We used the Avrami and the Arrhenius equations and the activation energy obtained at various experimental conditions. Although the crystallite size and TOP were increased with this alteration, AEPT of TiO_2 nanoparticles decreased when the gelatinization time increased. We suggest that a good morphology and low distribution of the anatase nanoparticles were another important factor that has contributed in the decrease of AEPT. In one word, TOP and AEPT of TiO_2 nanoparticles improved with the control of the morphology and the size due to the alteration of the calcination and the gelatinization time of the sol-gel route.

References

[1] Ahmad, A., Buzby, S., Ni, C., & Ismat. Shah, S. (2008). *J. Nanosci. Nanotechnol.*, *8*, 2410.
[2] Carp, O., Huisman, C. L., & Reller, A. (2004). *Prog. Solid State Chem.*, *32*, 33.
[3] Xiaobo, C., & Mao, S. S. (2007). *Chem. Rev.*, *107*, 2891.
[4] Diebold, U. (2003). *Surf. Sci. Rep.*, *28*, 53.
[5] Fujishima, A., & Honda, K. (1972). *Nature*, *238*, 37.
[6] Kaneko, M., & Okura, I. (2002). *Photocatalysis Science and Technology*, Springer press: Kodansha, Berline.
[7] Brown, W. D., & Granneman, W. W. (1978). *Solid State Electron.*, *21*, 837.
[8] Li, C., Zheng, Z., Zhang, F., Yang, S., Wang, H., Chen, L., Zhang, F., Wang, X., & Liu, X. (2000). *Nucl. Instrum. Methods Phys. Res., Sect. B*, *169*, 21.
[9] Kumazawa, N., Islam, M. R., & Takeuchi, M. (1999). *J. Electroanal. Chem.*, *472*, 137.
[10] Kavan, L., Fattakhova, D., & Krtil, P. (1999). *J. Electrochem. Soc.*, *146*, 1375.

[11] Bonini, N., Carotta, M. C., Chiorini, A., Guidi, V., Guidi, V., Malagu, C., Martinelli, G., Paglialonga, L., & Sacerdoti, M. (2000). *Sens. Actuators, B*, *68*, 274.
[12] Zhang, Q., & Gao, L. (1993). *Appl. Catal., B*, *3*, 37.
[13] Shen, Q., Katayama, K., Sawada, T., & Dupuis, M. (2007). *J. Phys. Chem. C*, *111*, 9290.
[14] Zumeta, I., Espinosa, R., Ayllon, J. A., Domenech, X., Rodriguez-Clemente, R., & Vigil, E. (2003). *Sol. Energy Mater. Sol. Cells*, *76*, 15.
[15] Lee, J. H., & Yang, Y. S. (2005). *J. Eur. Ceram. Soc.*, *25*, 3573.
[16] Zhu, Y., Zhang, L., Gao, C., & Cao, L. (2000). *J. Mater. Sci.*, *35*, 4049.
[17] Li, W., Ni, C., Lin, H., Huang, C. P., & Ismat Shah, S. (2004). *J. Appl. Phys.*, *96*, 6663.
[18] Picquart, M., Escobar-Alarcon, L., Torres, E., Lopez, T., & Haro-Poniatowski, E. (2002). *J. Mater. Sci.*, *37*, 3241.
[19] Mohammadi, M. R., Fray, D. J., & Mohammadi, A. (2008). *Micropor. Mesopor. Mat.*, *112*, 392.
[20] Yang, J., McCoy, B. J., & Madras, G. (2005). *J. Chem. Phys.*, *122*, 64901.
[21] Hu, Y., Tsai, H. L., & Huang, C. L. (2003). *Mater. Sci. Eng., A*, *344*, 209.